

## Numerical study of magneto-convective heat and mass transfer from inclined surface with Soret diffusion and heat generation effects: A model for ocean magnetohydrodynamics energy generator fluid dynamics

O. Anwar Bég<sup>1</sup>, T. A. Bég<sup>2</sup>, I. Karim<sup>3</sup>, M. S. Khan<sup>3</sup>, M. M. Alam<sup>3</sup>, M. Ferdows<sup>4</sup> and MD. Shamshuddin<sup>5\*</sup>

<sup>1</sup>Mechanical and Aeronautical Engineering, University of Salford, Manchester, M54WT, UK.

<sup>2</sup>Computational Mechanics and Renewable Energy Research, Dickenson Rd., Manchester, M13, UK.

<sup>3</sup>Mathematics Discipline, Science, Engineering and Technology, Khulna University, Khulna-9208, Bangladesh.

<sup>4</sup>College of Engineering and Science, Louisiana Tech University, Ruston, 71270, USA.

<sup>5\*</sup>Department of Mathematics, Vaagdevi College of Engineering, Warangal, Telangana, India.

\*Corresponding author: [shammaths@gmail.com](mailto:shammaths@gmail.com); [shamshuddin\\_md@vaagdevi.edu.in](mailto:shamshuddin_md@vaagdevi.edu.in)

### Research Highlights

1. A mathematical model is presented for MHD ocean generator inclined wall boundary layer flow with salinity, thermo-solutal buoyancy and heat generation.
2. Maple numerical quadrature solutions are validated with Nakamura and HAM methods.
3. Important thermophysical characteristics are studied of relevance to real systems.

### ABSTRACT

A mathematical model is developed for steady state magnetohydrodynamic (MHD) heat and mass transfer flow along an inclined surface in an ocean MHD energy generator device with heat generation and thermo-diffusive (Soret) effects. The governing equations are transformed into nonlinear ordinary differential equations with appropriate similarity variables. The emerging two-point boundary value problem is shown to depend on six dimensionless thermophysical parameters - *magnetic parameter, Grashof number, Prandtl number, modified Prandtl number, heat source parameter and Soret number in addition to plate inclination*. Numerical solutions are obtained for the nonlinear coupled ordinary differential equations for momentum, energy and salinity (species) conservation, numerically, using the Nachtsheim-Swigert shooting iteration technique in conjunction with the Runge-Kutta sixth order iteration scheme. Validation is achieved with Nakamura's implicit finite difference method. Further verification is obtained via the semi-numerical Homotopy analysis method (HAM). With an increase in magnetic parameter, skin friction is depressed

whereas it generally increases with heat source parameter. Salinity magnitudes are significantly reduced with increasing heat source parameter. Temperature gradient is decreased with Prandtl number and salinity gradient (mass transfer rate) is also reduced with modified Prandtl number. Furthermore, the flow is decelerated with increasing plate inclinations and temperature also depressed with increasing thermal Grashof number.

**KEYWORDS:** *Salinity, Soret number; MHD energy; Nakamura difference scheme; HAM.*

### NOMENCLATURE

$X, Y$	Cartesian coordinates (m)	$C_p$	Specific heat at constant pressure (J/kgK)
$G_r$	Grashof number	$\nu$	Kinematic viscosity ( $m^2/s$ )
$U, V$	Velocity components (m/s)	$\bar{\alpha}$	Heat source parameter
$P_s$	Modified Prandtl number	$\tau$	Dimensionless time (s)
$P_r$	Prandtl number	$f'(\eta)$	Dimensionless velocity component
$S_r$	Soret number	$\theta(\eta)$	Dimensionless temperature
$g$	Gravitational acceleration ( $m/s^2$ )	$\phi(\eta)$	Dimensionless salinity (concentration)
$F_s$	Molecular diffusivity	$\eta$	Similarity variable
$M$	Magnetic Parameter	$\beta$	Thermal expansion coefficient (/K)
$U_\infty$	Uniform velocity (m/s)	$\beta^*$	Thermal expansion coefficient due to salinity (/K)

## 1. INTRODUCTION

With the current state of energy resources in the world, the demand for sustainable renewable energy systems is ever-increasing. Many such systems have been developed and improved including photovoltaic solar collectors [1], re-charged geothermal reservoirs [2], wind turbines [3] and biomass [4]. The interest in *marine* energy systems has also been considerable (particularly in Asia) and among the many robust methodologies which have been developed are OTEC (ocean thermal energy conversion) [5], tidal power stations [6] and wave energy conversion devices [7]. Although many different marine renewable designs have been propounded, a particularly exciting and feasible initiative has been the MHD (magnetohydrodynamic) seawater generator [8]. This device transforms kinetic energy of the ocean/tidal current into electrical energy via the MHD principle [9]. In MHD ocean generators, as with conventional land-based MHD power generators, the applied magnetic field is a key factor in optimizing efficiency and performance. Many different systems have been studied including rotating channels [10], Hall current generators [11], helicoid generators exploiting superconducting magnets

[12] and rotating disk MHD generators [13]. The need to further understand the intricate characteristics of momentum, heat and mass (salinity) transport in these systems, as a means of further enhancing operational efficiency, has motivated substantial interest in mathematical and computational modeling. Temperature, pressure, and salinity are three important properties of sea water, and they determine the physical properties associated with sea wave motion. The presence of small suspended particles in sea water also exerts an important influence on sea water power generation [14].

Inclined magnetofluid dynamic flows with and without heat and mass transfer have received significant attention in recent years. These studies have considered numerous multiphysical effects of relevance to energy generator systems. Srikanth et al. [15] studied radiative flux effects on magnetized nanofluid convection flow from a porous inclined plate. Ramesh et al. [16] investigated Chandrasekhar (magnetic) number and heat generation/absorption effects on hydromagnetic convection in a fluid-particle suspension boundary layer flow from a stretching plate. Kabir and Al Mahbub [17] examined thermophoresis effects on transient double-diffusive magneto-convection from an inclined plane. Palani and Kim [18] used a finite difference technique to obtain solutions for hydromagnetic dissipative natural convection flow from a tilted non-isothermal plate with Ohmic heating effects. Chamkha et al. [19] used the Blottner difference method to study buoyancy-driven magneto-convection along a plate in porous media with thermal (solar) radiative flux. Masthanrao et al. [20] examined chemical reaction effects on steady two-dimensional hydromagnetic free convection along an inclined plate adjacent to a permeable regime with wall transpiration. Hossain et al. [21] used local similarity and finite difference procedures to study weak magnetic field effects on inclined plate convection. Ramadan and Chamkha [22] studied computationally the two-phase natural convection magnetized boundary layer flow from inclined surfaces with variable properties. Wang and Chen [23] used a cubic spline alternating-direction implicit method to simulate mixed convection magnetohydrodynamic flow from an inclined wavy plate, showing that heat transfer rate and the skin-friction coefficient are depressed with increasing plate inclination. Furthermore, they observed that increasing magnetic body force accelerates the flow near the leading edge of the wavy surface whereas it decelerates the flow far downstream of the leading edge. Chen [24] investigated momentum, heat and mass transfer characteristics of non-isothermal, non-iso solutal hydromagnetic natural convection from a porous inclined surface with Joule and viscous dissipation.

The above studies have generally ignored simultaneous species diffusion (mass transfer). However as noted earlier, salinity in ocean MHD generators [9] is a critical issue and it is important to investigate the coupled effects of heat and mass transfer in transport in such devices. Mass diffusion follows the Fickian law [25] and introduces some complex characteristics in mixed convection flows. Recent studies include Ferdows et al. [26] who reported on wall slip effects in double-diffusive convection and Rashidi et al. [27] who employed group methods to study reactive boundary layer convective transport phenomena. Interesting studies include Zueco et al. [28] who used network simulation to analyze variable thermophysical effects in thermophoretic magneto-convection. [29]. These studies however omitted thermal –diffusion (*Soret*) or diffuso-thermal (*Dufour*) effects. The former is a phenomenon which has been known to physicists for over a century and has significant applications in chromatography, binary-fluid systems, energy generators and many other industrial processes. Abreu et al. [30] obtained Adomian polynomial-based solutions for laminar boundary layer flows in forced and natural convection with cross diffusion effects. Bég et al. [31] showed that the Soret effect dominates the Dufour effect in mixed convection from inclined plates using a local non-similarity method and boundary layer theory. Bég and Tripathi [32] demonstrated the important influence of Soret thermo-diffusion on peristaltic propulsion in deformable channels using Mathematica. They further described the subtle relationship between buoyancy forces, wave amplitude and both Soret and Dufour effects. Many other studies have been communicated evaluating the influence of cross-diffusion on double-diffusive boundary layer flows. These include Coelho and Telles [33] who considered the Graetz problem and Bég et al. [34] who studied the magnetohydrodynamic Sakiadis flow in a porous medium. Bég et al. [35] further investigated the micromorphic transport in a porous medium with cross-diffusion using a variational finite element method. Vasu et al. [36] investigated Soret and Dufour effects on hydromagnetic transport from a spherical body in porous media. Very recently Vasu et al. [37] also presented robust finite difference solutions for transpiration (lateral mass flux) effects on Soret-Dufour cross diffusion in laminar gas dynamic flows. These studies all confirmed that Soret/Dufour effects are significant when density differences exist in the flow regime. In addition, these studies have emphasized that when heat mass transfer occur simultaneously in a moving fluid, an energy flux is produced not only due to temperature gradients but also via concentration gradients (“composition gradients”). The energy flux induced by the concentration gradient is termed the Dufour or diffusion-thermo effect. The mass flux generated via temperature gradients is the Soret or thermo-diffusion effect.

The afore-mentioned studies have not considered *inclined-plate* MHD flows with Soret and heat generation effects. Therefore, in the present study we examine the transport phenomena from an *inclined surface* in an MHD ocean generator with heat generation and also thermo-diffusion effects. The *Soret effect* is included as it is known to be prominent in saltwater solution transport phenomena. We develop a laminar steady-state boundary layer model for magnetohydrodynamic double-diffusive convection in seawater flow along an inclined non-conducting plate with heat generation present. The governing equations are transformed into a system of coupled, nonlinear ordinary differential equations which are shown to be controlled by several thermophysical parameters, namely a magnetic body force parameter ( $M$ ), Grashof number ( $G_r$ ), Prandtl number ( $P_r$ ), modified Prandtl number ( $P_s$ ), a heat source parameter ( $\bar{\alpha}$ ) and the Soret number ( $S_r$ ) in addition to the plate inclination. Heat generation has been shown to be an important consideration in energy systems and has been studied in recent papers by Bég *et al.* [38] and Uddin *et al.* [39]. Here we utilize the Nactsheim-Swigert shooting iteration technique together with Runge-Kutta six order iteration schemes available in Maple to solve the nonlinear boundary value problem. Furthermore, we validate the computations with a separate implicit finite difference code based on Nakamura's method [40] with the MAG-NAK code. Further validation is attained via series solutions using the powerful semi-numerical homotopy analysis method (HAM). The velocity, temperature and salinity (species concentration) distributions are computed for a wide spectrum of the control parameters. Additionally, skin-friction coefficient, surface heat transfer and salinity (mass transfer) rates are also computed. The study is relevant to MHD seawater energy generators.

## 2. MATHEMATICAL TRANSPORT MODEL

MHD ocean generators offer a feasible potential for humanity. Many pioneering investigations into this form of renewable energy have been conducted by Russian, French, American and Japanese engineers. The fundamental principle of MHD ocean energy generation in which seawater is the working fluid and the applications may include floating installations or propulsion systems, are summarized with a possible design for a floating MHD ocean energy installation in Japan and additionally the physical model for the current flow to be studied with the coordinate system in **Fig. 1**. A two-dimensional simplified model is considered of the near-wall flow in such a system. The  $X$ -axis is directed along the

generator channel wall and the boundary layer flow is upward; the  $Y$ -axis is inclined to it. Here  $\alpha$  is the angle of inclination. Initially it is assumed that the plate as well as the fluid is at the same temperature,  $T_\infty$ , and the salinity level  $S_\infty$  everywhere in the fluid is same.

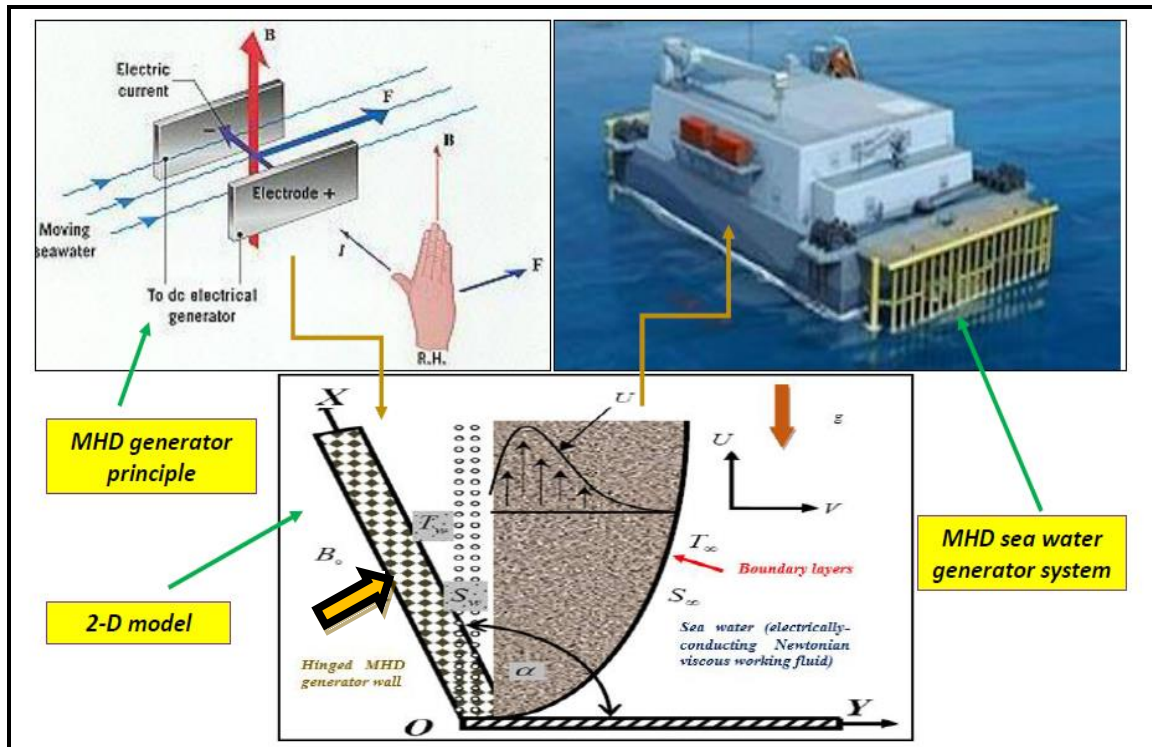


**Fig 1:** MHD ocean energy generation principle with conceptual floating MHD energy generator and simplified 2-dimensional physical model for inclined duct wall system.

Also, it is assumed that the fluid and the generator channel wall (plate) is at rest; subsequently the wall moves with a constant velocity along the  $X$ -direction. The temperature of the wall and species salinity are raised to  $T_w (> T_\infty)$  and  $S_w (> S_\infty)$  respectively, and these are sustained thereafter, where  $T_w, S_w$  are temperature and species salinity at the wall and  $T_\infty, S_\infty$  are the temperature and salinity of the species far away from the wall, respectively. Weak magnetic field is considered and therefore Hall currents are neglected as is Joule (Ohmic) heating and viscous dissipation. A magnetic field,  $B_o$ , is applied in the  $Y$ -direction. The magnetic field is always perpendicular to the wall. The magnetic field applied is always orientated at 90 degrees to the wall. Therefore, while the wall can change in orientation, the magnetic field does not. The Lorentz force is as such always in the same direction relative to wall (plate). Under the boundary layer approximation with the Boussinesq assumption, the governing equations for mass, momentum, species (salinity) and

energy conservation, incorporating heat generation and Soret effects, may be shown to take the form:

**Continuity equation (Mass Conservation):**

$$\frac{\partial U}{\partial X} + \frac{\partial V}{\partial Y} = 0, \quad (1)$$

**Momentum Conservation:**

$$\left( U \frac{\partial U}{\partial X} + V \frac{\partial U}{\partial Y} \right) = \nu \left( \frac{\partial^2 U}{\partial Y^2} \right) + g\beta(T - T_\infty)\sin\alpha - \frac{\sigma B_o^2}{\rho} U, \quad (2)$$

**Species (Salinity) Conservation:**

$$\left( U \frac{\partial S}{\partial X} + V \frac{\partial S}{\partial Y} \right) = K_s \left( \frac{\partial^2 S}{\partial Y^2} \right) + F_s \left( \frac{\partial^2 T}{\partial Y^2} \right) \quad (3)$$

**Energy (Heat) Conservation:**

$$\left( U \frac{\partial T}{\partial X} + V \frac{\partial T}{\partial Y} \right) = K_T \left( \frac{\partial^2 T}{\partial Y^2} \right) + \frac{Q_T}{\rho C_p} \quad (4)$$

The prescribed boundary conditions are:

$$\begin{aligned} \text{At } Y = 0: & U = V = 0; T = T_w = T_\infty + \sin\alpha; S = S_w = S_\infty + \sin\alpha \\ \text{As } Y \rightarrow \infty: & U \rightarrow 0, V \rightarrow 0, T \rightarrow T_\infty, S \rightarrow S_\infty \end{aligned} \quad (5)$$

Here  $\nu$  is the kinematic viscosity,  $B_o$  is the magnetic field strength,  $K_s = K / \rho C_s$  is the thermal diffusivity due to salinity (salt species),  $K_T = K / \rho C_p$  is the thermal diffusivity due to temperature,  $F_s$  is the molecular diffusivity,  $C_p$  is the specific heat at constant pressure,  $U$  is the uniform velocity,  $\sigma$  is the electrical conductivity of the fluid,  $g$  is the acceleration due to earth gravity,  $\beta$  is the volumetric thermal expansion coefficient,  $\beta^*$  is the mass expansion coefficient,  $Q_T = (T - T_\infty)Q^*$  is the heat generation and  $\rho$  is the density of the fluid. The penultimate term in eqn. (3) is the Soret thermo-diffusion term (mass diffusion generated via

temperature gradients). It is important to note that the thermal and solutal boundary conditions enforced in Eqn. (5) do reflect the inclusion of plate orientation on the temperature and solutal (species concentration) fields, and follow the methodology of Gebhart *et al.* [41]. They are however not *non-isothermal* or *non-isosolutal* since there is no variation with streamwise coordinate. This may provide future refinement in the model but is neglected in the current study. Thermal and species effects at the wall can never be completely controlled especially in MHD ocean generator environments. However, it is not possible to mimick the full spatial or time variation of such phenomena with the current fluid dynamics methodology. To develop a robust boundary value problem, engineers must make some logical and validated assumptions, and these have been founded on boundary-layer theory following Gebhart *et al.* [41]. This provides a reasonable approximation for near-wall transport phenomena. The boundary value problem defined by the eqns. (1)-(4) under boundary conditions (5) cannot be solved analytically. In primitive variables, numerical solutions are the only feasible option. However even numerical solutions of the primitive boundary value problem (e.g. with finite element or finite difference techniques) do not yield solutions in terms of important *dimensionless variables*. In order to achieve this, we introduce similarity transformations next to render the problem dimensionless and thereby also convert the system from a *partial differential equation* one to an *ordinary differential equation* one. This greatly simplifies the numerical solution and simultaneously retains many important physical aspects of the transport phenomena under investigation.

### 3. TRANSFORMATION OF MODEL

Proceeding with the analysis, we define the following dimensionless variables:

$$\eta = y \sqrt{\frac{U_o}{2\nu X}}, \psi = \sqrt{2\nu U_o X} f(\eta), \theta = \theta(\eta) = \frac{T - T_\infty}{T_w - T_\infty}, \phi = \phi(\eta) = \frac{S - S_\infty}{S_w - S_\infty}$$

$$u = \frac{\partial \psi}{\partial Y}, \quad v = -\frac{\partial \psi}{\partial X} \quad (6)$$

All parameters are defined in the notation section. Introducing these into eqns. (1)-(4) yields the following system of non-dimensional, non-linear coupled, ordinary differential equations:

$$f''' + ff'' + Gr\theta \sin \alpha - Mf' = 0 \quad (7)$$

$$\theta'' + Pr f\theta' + Pr \bar{\alpha}\theta = 0 \quad (8)$$

$$\phi'' + P_s f \phi' + P_s S_r \theta'' = 0 \quad (9)$$

The boundary conditions reduce to:

$$\begin{aligned} \text{At } \eta = 0: f = 0; f' = 0, \theta = \sin \alpha, \phi = 1 \\ \text{As } \eta \rightarrow \infty: f' \rightarrow 0, \theta \rightarrow 0, \phi \rightarrow 0 \end{aligned} \quad (10)$$

where the primes denote differentiation with respect to  $\eta$  and  $G_r = 2g\beta(T_w - T_\infty)X/U_o^2$  is thermal Grashof number,  $M = 2\sigma\beta_o^2 X/U_o$  is the local magnetohydrodynamic body force parameter,  $P_r = \nu\rho C_p/K$  is the Prandtl number,  $P_s = \nu\rho C_s/K$  is the modified Prandtl number,

$$\bar{\alpha} = 2XQ^*/U_o\rho C_p \text{ is the heat generation (source) parameter, } S_r = \frac{F_s}{\nu} \left( \frac{T_w - T_\infty}{S_w - S_\infty} \right) \text{ is the Soret}$$

(thermo-diffusion) number. The engineering design functions of interest in energy systems are the surface shear stress (skin-friction coefficient), the *Nusselt number* (heat transfer rate) and *Sherwood number* (salinity transfer rate) which are computed respectively by the following expressions:

$$\begin{aligned} C_f (Re)^{-1/2} &= -f''(0) \\ N_u (Re)^{-1/2} &= -\theta'(0) \\ S_h (Re)^{-1/2} &= -\phi'(0) \end{aligned} \quad (11)$$

where  $Re$  is the local Reynolds number.

## 4. NUMERICAL SOLUTIONS

Here we describe the numerical methods employed to solve the derived nonlinear boundary value problem. These are Maple quadrature, Nakamura's tridiagonal finite difference scheme (NTS) and the homotopy analysis method (HAM). Each method is described in due course.

### 4.1 Maple Quadrature

The two-point BVP defined by the non-linear, coupled ordinary differential equations (7) to (9) with boundary conditions (10) are solved numerically using the Nactsheim-Swigert shooting iteration technique [42] with a Runge-Kutta six order iteration scheme available in MAPLE. Initially velocity, temperature and salinity are determined as functions of the transverse dimensionless coordinate,  $\eta$ . Extension of the iteration shell to above equation

system of differential equations (10) is straightforward—there are three asymptotic boundary conditions and hence three unknown surface conditions,  $f'(0)$ ,  $\theta(0)$  and  $\phi(0)$ . Very fast and efficient computations are achieved on a Laptop. It is important to note that in the numerical simulations, as far as possible, precise data has been used based on actual working MHD systems described in Rosa [43] and Li *et al.* [44]. Thermal data and all other parameters (Soret number, Grashof number, heat generation parameter, Prandtl number) have been based on the extensive information available in Gebhart *et al.* [41]. The parameter ranges selected therefore apply to seawater scenarios under a static magnetic field with incompressible, viscous approximations, consistent with the boundary-layer approach. Furthermore, the correct scaling of the magnetic parameter ( $M$ ) has been achieved in consistency with viable seawater electrical conductivity, magnetic field strengths and viscosity properties for high efficiency systems.

#### 4.2 Validation with Nakamura Finite Difference Method

To verify the Maple solutions, the well-posed nonlinear two-point boundary value problem has also been solved with the efficient implicit Nakamura Tridiagonal finite difference Scheme (NTS), introduced in a seminal article by Nakamura [41]. A recent review of numerous applications of Nakamura's technique in nonlinear magnetohydrodynamic transport phenomena has been presented by Bég [45]. The MAG-NAK code has been developed to implement the Nakamura method for *magnetofluid* dynamics problems. As with other difference schemes, a reduction in the higher order differential equations, is also fundamental to this method. It is also particularly effective at simulating highly nonlinear flows as characterized by coupled heat and mass transfer problems. Interesting applications utilizing the Nakamura scheme include micromorphic flows [46], magneto-micropolar rheological heat transfer [47], magnetic combustion [48] and nanofluid bioconvection transport in biomimetic fuel cells [49]. NTS works well for both one-dimensional (ordinary differential) and two-dimensional (partial differential) non-similar flows. NTS entails a combination of the following aspects.

- The flow domain for the regime is discretized using an *equi-spaced* finite difference mesh in the  $\eta$  direction.
- The partial derivatives for  $f$ ,  $\theta$ ,  $\phi$ , with respect to  $\eta$  are evaluated by central difference

approximations.

- A single iteration loop based on the method of successive substitution is utilized due to the high nonlinearity of the momentum, energy and salinity (species) conservation equations.
- The finite difference discretized equations are solved as a linear second order boundary value problem of the ordinary differential equation type on the  $\eta$  domain.

For the energy conservation and salinity eqns. (8, 9) which are *second order* equations, only a *direct* substitution is needed. However, a reduction is required for the momentum eqn. (7) which is third order. Setting:

$$P = f' \tag{12a}$$

$$Q = \theta \tag{12b}$$

$$R = \phi \tag{12c}$$

The eqns. (7)-(9) then assume the form:

***Nakamura momentum equation:***

$$A_1 P'' + B_1 P' + C_1 P = S_1 \tag{13}$$

***Nakamura energy equation:***

$$A_2 Q'' + B_2 Q' + C_2 Q = S_2 \tag{14}$$

***Nakamura salinity (species) equation:***

$$A_3 R'' + B_3 R' + C_3 R = S_3 \tag{15}$$

where  $A_{i=1...3}$ ,  $B_{i=1...3}$ ,  $C_{i=1...3}$  are the *Nakamura matrix coefficients*,  $S_{i=1...3}$  are the *Nakamura source terms* containing a mixture of variables and derivatives associated with the lead variable. The Nakamura eqns. (13)-(15) are transformed to finite difference equations and these are formulated as a “tridiagonal” system which is solved iteratively. Tables 1-3 also compare the Nakamura solution with the Maple solutions for the salinity (species concentration), skin friction and temperature gradient functions at selected values of the heat source parameter. In all cases, excellent agreement is observed. Confidence in the present **Maple** computations, which are used for all graphical depictions, is therefore very high.

Approximately 300 domain points along the  $\eta$ -direction were required to achieve the necessary accuracy. Lesser domain points do not converge correctly or sufficiently and experiments with 100, 150, 200, 250 grid points were found to be unsatisfactory.

### 4.3 Further Validation with Homotopy Analysis Method (HAM)

The 7<sup>th</sup> order coupled nonlinear ordinary differential boundary value problem defined by equations (7)–(10) has also been solved by the homotopy analysis method (HAM). Liao [50] developed HAM via homotopy in topology to generate a general analytical-numerical method for nonlinear problems. The validity of HAM is independent of whether or not there exist small parameters in the considered equation(s). Therefore HAM can overcome the foregoing restrictions of perturbation methods. In recent years, HAM has been successfully employed to solve many non-linear problems in engineering sciences including smart biological lubrication [51] and nanofluid energy systems [52]. Denoting  $f=F$ ,  $\theta=G$ ,  $\phi=H$ , in HAM we write the initial guesses and linear operators as:

$$F_0(\eta) = \eta - 1 + e^{-\eta}, \quad G_0(\eta) = e^{-\eta}, \quad H_0(\eta) = e^{-\eta}, \quad (16a)$$

$$L_F = \frac{d^3 F}{d\eta^3} - \frac{dF}{d\eta}, \quad L_G = \frac{d^2 G}{d\eta^2} - G, \quad L_H = \frac{d^2 H}{d\eta^2} - H, \quad (16b)$$

with the following properties:

$$\begin{aligned} L_F(C_1 + C_2 e^\eta + C_3 e^{-\eta}) &= 0, & L_G(C_4 e^\eta + C_5 e^{-\eta}) &= 0, \\ L_G(C_6 e^\eta + C_7 e^{-\eta}) &= 0, & L_N(C_8 e^\eta + C_9 e^{-\eta}) &= 0, \end{aligned} \quad (17)$$

where  $C_i$  ( $i=1-9$ ) are arbitrary constants. Let  $q \in [0, 1]$  represent an embedding parameter and  $\hbar_F, \hbar_G, \hbar_H, \hbar_N$  denote the nonzero auxiliary linear operators and construct the following zeroth order deformation equations:

$$(1-q) L_f [\hat{F}(\eta; q) - F_0(\eta)] = q \hbar_F N_F^* [\hat{F}(\eta; q)], \quad (18)$$

$$(1-q) L_G [\hat{G}(\eta; q) - G_0(\eta)] = q \hbar_G N_G^* [\hat{G}(\eta; q), \hat{F}(\eta; q)], \quad (19)$$

$$(1-q) L_H [\hat{H}(\eta; q) - H_0(\eta)] = q \hbar_H N_H^* [\hat{H}(\eta; q), \hat{F}(\eta; q)], \quad (20)$$

$$(1-q) L_N \left[ \hat{N}(\eta; q) - N_0(\eta) \right] = q \hbar_N N_N^* \left[ \hat{N}(\eta; q), \hat{F}(\eta; q) \right], \quad (21)$$

The *transformed boundary conditions* are *non-linear operators* may then be defined. Taylor expansions of the approximations are then conducted, and auxiliary parameters are properly selected to achieve fast convergence of these series. The resulting problems at the  $m^{\text{th}}$  order deformation are then formulated with associated boundary conditions and eventually a general solution of the Eqns. (7)-(9) is achieved in which  $F_m^*(\eta)$ ,  $G_m^*(\eta)$ ,  $H_m^*(\eta)$  are the particular solutions and the constants are to be determined by the boundary conditions. HAM achieves an analytical solution of the problem in series form. An important consideration is convergence of the series solution given by HAM which depends strongly upon auxiliary parameters  $\hbar_F$ ,  $\hbar_G$ ,  $\hbar_H$ . These parameters provide a *convenient mechanism* for adjusting and controlling the convergence region and convergence rate of the series solution. Therefore, in order to select appropriate values for these auxiliary parameters, the so called  $\hbar_F$ ,  $\hbar_G$ ,  $\hbar_H$  curves are computed at 20<sup>th</sup> order approximations, to guarantee exceptional accuracy, and are therefore adopted in all HAM numerical computations. The comparison of solutions via Maple shooting quadrature and HAM is also provided in **Tables 1-3**. Again, excellent correlation is achieved with both Maple and NTS. Confidence in the Maple solutions is therefore very high.

**Table 1:** Maple, NTS and HAM solutions for salinity function (species concentration) with  $\bar{\alpha} = 0.5$ ,  $M = 1.0$ ,  $G_r = 4.0$ ,  $P_r = 0.5$ ,  $P_s = 1.0$ ,  $S_r = 1.0$  and  $\alpha = 90^\circ$  (vertical plate).

$\eta$	$\phi$ [Maple]	$\phi$ [NTS]	$\phi$ [HAM]
0.0	1.0000	1.0000	1.0000
0.25	0.8821	0.8823	0.8821
0.50	0.6473	0.6474	0.6473
0.75	0.2397	0.2393	0.2395
1.0	0.0000	0.0000	0.0000

**Table 2:** Maple, NTS and HAM solutions for skin friction with  $M = 2.0$ ,  $G_r = 1.0$ ,  $P_r = 0.125$ ,  $P_s = 10.0$ ,  $S_r = 1.0$  and  $\alpha = 45^\circ$  (inclined plate).

$\bar{\alpha}$	$-f''(0)$ [Maple]	$-f''(0)$ [NTS]	$-f''(0)$ [HAM]
0.1	1.0000	1.0000	1.0000

0.2	0.8821	0.8823	0.8824
0.3	0.6473	0.6474	0.6475
0.4	0.2397	0.2393	0.2394
0.5	0.0000	0.0000	0.0000

**Table 3:** Maple, NTS and HAM solutions for heat transfer rate (Nusselt number function) with  $M = 1.0$ ,  $G_r = 4.0$ ,  $P_r = 1.0$ ,  $P_s = 1.0$ ,  $S_r = 1.0$  and  $\alpha = 45^\circ$  (inclined plate).

$\bar{\alpha}$	$-\theta'(0)$ [Maple]	$-\theta'(0)$ [NTS]	$-\theta'(0)$ [HAM]
0.1	0.0503	0.0502	0.0501
0.2	0.1604	0.1605	0.1604
0.3	0.2254	0.2256	0.2257
0.4	0.3212	0.3213	0.3214
0.5	0.3813	0.3815	0.3816

With regard to the relative performance of the three numerical techniques employed for the nonlinear ordinary differential boundary value problem, the best solution convergence was achieved with the 20<sup>th</sup>-order HAM approximation. We have compared the compilation times for the three methods and also percentage errors in **Tables 4, 5 and 6** for the salinity function (species concentration), skin friction and Nusselt number function, respectively (corresponding to the computations for  $\bar{\alpha} = 0.5$  in Tables 1, 2 and 3 respectively). This provides a good insight into relative performance. Maple was found to be the fastest solver, however the error % was marginally higher compared with NTS whereas the best accuracy unquestionably is achieved with HAM. However, HAM requires considerably more algebraic analysis in determining the correct  $m^{\text{th}}$  order deformation equation and is much more rigorous and time-consuming to set up. Overall the other two methods (Maple and NTS) are faster to program and do achieve sufficiently high accuracy and impressive compilation times. NTS is in fact easier to program and has second order accuracy. All computations were executed on a Lenovo Y510p laptop machine with 8 GB of RAM and an Intel® Core i7-4700MQ CPU @ 2.4 GHz processor running on a Windows 10 platform.

**Table 4:** Maple, NTS and HAM relative numerical performance for salinity function (species concentration) with  $\bar{\alpha} = 0.5$ ,  $M = 1.0$ ,  $G_r = 4.0$ ,  $P_r = 0.5$ ,  $P_s = 1.0$ ,  $S_r = 1.0$  and  $\alpha = 90^\circ$  (vertical plate).

NUMERICAL METHOD	MAPLE	NTS	HAM
Compilation time (s)	150	160	310
% Error	2.1%	3.2%	0.5%

**Table 5:** Maple, NTS and HAM relative numerical performance for skin friction with  $\bar{\alpha} = 0.5$ ,  $M = 2.0$ ,  $G_r = 1.0$ ,  $P_r = 0.125$ ,  $P_s = 10.0$ ,  $S_r = 1.0$  and  $\alpha = 45^\circ$  (inclined plate).

NUMERICAL METHOD	MAPLE	NTS	HAM
Compilation time (s)	170	190	340
% Error	2.5%	2.7%	1.3 %

**Table 6:** Maple, NTS and HAM relative numerical performance for heat transfer rate (Nusselt number function) with  $\bar{\alpha} = 0.5$ ,  $M = 1.0$ ,  $G_r = 4.0$ ,  $P_r = 1.0$ ,  $P_s = 1.0$ ,  $S_r = 1.0$  and  $\alpha = 45^\circ$  (inclined plate).

NUMERICAL METHOD	MAPLE	NTS	HAM
Compilation time (s)	135	147	305s
% Error	1.8%	1.9%	0.8%

## 5 RESULTS AND DISCUSSION

Following extensive verification of the accuracy of the Maple numerical quadrature approach, Maple has been selected as the method used to compute velocity ( $f'$ ), temperature ( $\theta$ ) and salinity ( $\phi$ ) variations for the effects of magnetohydrodynamic body force parameter ( $M$ ), Grashof number ( $G_r$ ), Prandtl number ( $P_r$ ), modified Prandtl number ( $P_s$ ), heat generation parameter ( $\bar{\alpha}$ ) and Soret number ( $S_r$ ) at different plate inclinations ( $\alpha$ ). These are

illustrated in **figs. 2-8**. A significant depression in velocity (Figs. 2 and 3) accompanies a rise in Grashof number for some distance from the plate surface into the boundary layer.  $G_r = 2g\beta(T_w - T_\infty)X / U_o^2$  and this parameter simulates the relative effect of buoyancy force (free convection) to viscous force in the regime. For  $Gr > 1$ , *buoyancy force* dominates the *viscous force*. Increasing buoyancy therefore decelerate the flow closer to the plate surface. With greater inclination angle ( $\alpha = 120^\circ$  in fig.3 compared with  $\alpha = 90^\circ$  in fig. 2) there is a decrease in velocity magnitudes. Referring to Fig. 1 this implies that a vertical plate ( $\alpha = 90^\circ$ ) achieves better flow acceleration under thermal buoyancy than an inclined plate ( $\alpha = 120^\circ$ ). This follows logically from inspection of the dimensionless momentum Eqn. (7) wherein the buoyancy force, viz,  $+Gr\theta\sin\alpha$  is clearly directly proportional to the linear product of Gr,  $\sin\alpha$  and  $\theta$ . Clearly as  $\sin 90 (=1) > \sin 120 (=0.8660)$  then the buoyancy force will be lower for the same Grashof number. The inclined plate buoyancy force will be exceeded by the vertical plate buoyancy force and this will result in deceleration in the former. *Plate orientation is therefore a critical geometric parameter which can be exploited to manipulate transport characteristics in the MHD ocean generator system.*

**Fig. 4** illustrates the influence of the heat source parameter ( $\bar{\alpha}$ ) on salinity (concentration) distributions with transverse coordinate. Increasing heat generation clearly depresses concentration values. The removal of thermal energy in the regime decreases the intensity of thermal convection and this in turn suppresses species diffusion in the boundary layer. This has also been observed in other magnetohydrodynamic flows [38] and even in non-Newtonian nanofluid flows [39]. Salinity boundary layer thickness is therefore also reduced with larger values of the heat source parameter. This simple mechanism, as further elucidated by Haajizadeh *et al.* [53] exerts a dramatic influence on the transport of heat in boundary layer flows and thereby significantly also effects the diffusion of salinity. In practical MHD ocean energy generators, heat generation can be introduced by spot pulse heating [8, 9] and may be used to regulate salinity levels in seawater flows being conveyed to the conversion mechanism. Although not computed, it is anticipated that heat absorption ( $\bar{\alpha} < 0$ ) will induce the reverse effect.

**Fig. 5** illustrates the influence of thermal Grashof number ( $G_r$ ) on temperature evolution. with transverse coordinate,  $\eta$ . Increasing buoyancy effect as represented via an increase in Grashof number, significantly depresses the temperature magnitudes at the plate and in close vicinity to it- in fact negative temperatures are induced. However, with further distance from the plate surface into the free stream, there is a slight elevation in the temperature indicating

that thermal boundary layer thickness is enhanced with stronger buoyancy effect there. Thermal buoyancy therefore is an important feature of realistic MHD generator flows and properly characterizes natural convection effects which arise in such systems. Neglect of this phenomenon (forced convection”) leads to erroneous predictions of temperature fields and ultimately inaccurate efficiency predictions for working systems.

**Fig. 6** illustrates the influence of magnetohydrodynamic body force parameter ( $M$ ) on skin friction (surface shear stress function) distributions, with heat source parameter ( $\bar{\alpha}$ ) for the *vertical* plate case ( $\alpha = 90^\circ$ ). Increasing  $M$  clearly generates a strong depression in skin friction, since larger  $M$  is associated with greater Lorentzian magnetohydrodynamic drag force. This drag acts transverse to the applied magnetic field and significantly impedes the boundary layer flow and results in an increase in momentum boundary layer thickness. Magnetic field therefore achieves a damping effect. The trend is consistent with many other studies of hydromagnetic boundary layers including Doss and Roy [12] and Palani *et al.* [18]. The case of  $M = 0.0$  corresponds to vanishing hydromagnetic effect (electrically non-conducting fluid) and  $M = 1$  implies an equivalence of magnetic drag force and inertial body force in the boundary layer regime. The skin friction in fig. 6 is conversely observed to be boosted with increasing heat generation effect i.e. the flow is accelerated with increasing parameter  $\bar{\alpha}$  values, at all values of the magnetic parameter.

**Fig. 7** shows the effect of modified Prandtl number ( $P_s$ ) on salinity (mass transfer) rates (i.e. Sherwood number function) also plotted against heat source parameter ( $\bar{\alpha}$ ) for the obtuse plate case ( $\alpha = 120^\circ$ ). A substantial decrease in  $-\phi'$  magnitudes accompanies an increase in ( $P_s$ ); however, this is only at large values of heat generation parameter. For lower values of heat generation, there is only a slight reduction in the salinity gradient profiles with a very large increase in modified Prandtl number. Effectively therefore when heat source is strong, the salinity (concentration) boundary layer thickness will be depleted. The inclusion of salinity in the model therefore has a non-trivial contribution. Many MHD generator studies neglect mass (salinity) diffusion and the current study confirms that this is an important phenomenon which should be included to properly predict actual fluid dynamic characteristics of real MHD ocean energy generators since they operate in a seawater environment, as further corroborated by Rosa [43]

**Fig. 8** finally presents the temperature gradient shows the effect of ordinary Prandtl number ( $P_r$ ) on Nusselt number function profiles (heat transfer gradients), once again versus

heat source parameter ( $\bar{\alpha}$ ), also for the obtuse plate case ( $\alpha = 120^\circ$ ). Nusselt number magnitudes are evidently lowered with increasing Prandtl number, especially at higher heat source values.  $Pr$  represents the ratio of momentum diffusivity to thermal diffusivity in the boundary layer regime.  $Pr < 1$  physically corresponds to cases where heat diffuses faster than momentum and vice versa for  $Pr > 1$ .  $Pr = 0.7$  is an accurate value for water-based solvents and  $Pr \gg 1$ , e.g., 7, is associated with seawater. Greater  $Pr$  will also reduce thermal boundary layer thickness. Smaller  $Pr$  fluids possess higher thermal conductivities so that heat can diffuse away from the cone surface (wall) faster than for higher  $Pr$  fluids (thicker boundary layers). Our computations show that a rise in  $Pr$  depresses the temperature function and therefore also the Nusselt number (less heat is transferred from the plate to the fluid). This concurs with many other simulations of hydromagnetic convection including Masthanrao [20], Hossain *et al.* [21] etc. Relative rates of thermal and momentum diffusion are controlled by the Prandtl number. This parameter is therefore a critical consideration in robust MHD ocean generator design and an automatic control system may be utilized to control plate orientation.

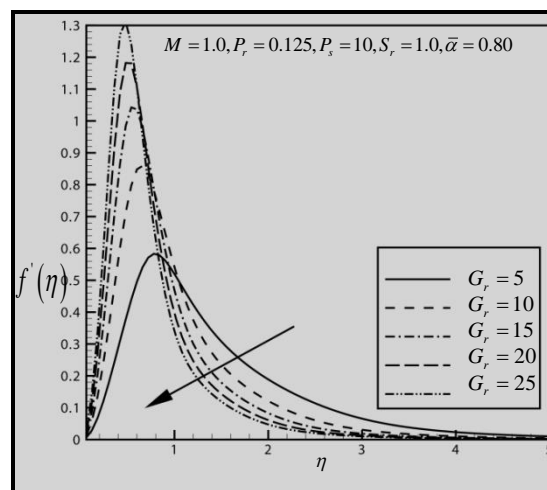


**Fig.2.** Effect of Grashof number on velocity distributions for plate inclination angle ( $\alpha=90^\circ$ ) (vertical plate).

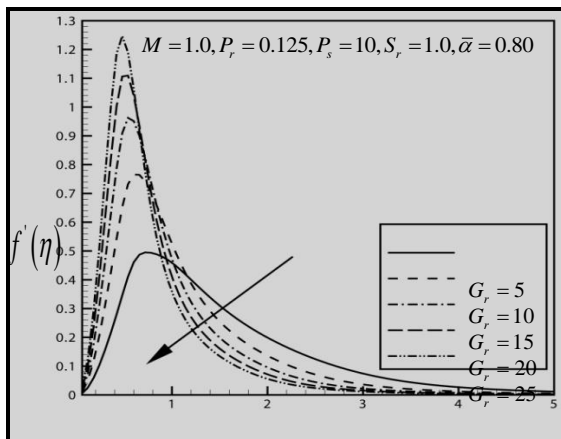


**Fig. 3.** Effect of Grashof number on velocity distributions for plate inclination angle ( $\alpha=120^\circ$ ).

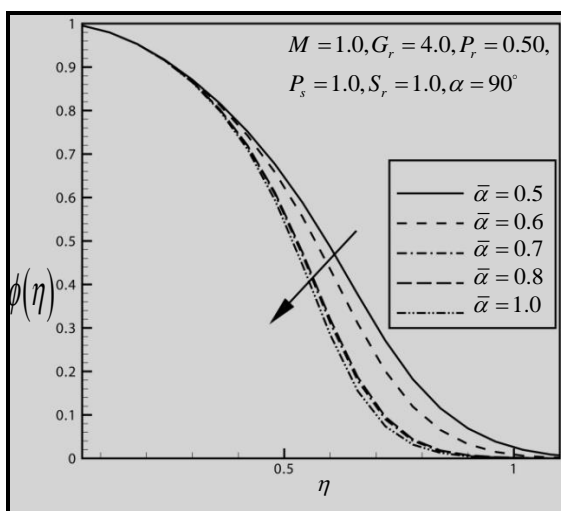


**Fig.4.** Effect of heat source parameter ( $\bar{\alpha}$ ) on salinity profiles.

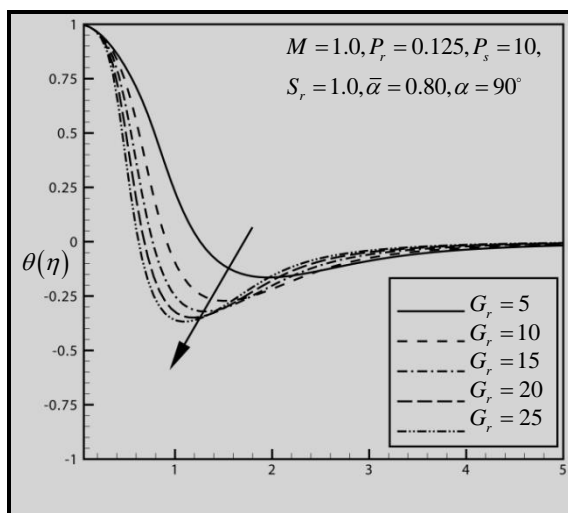


**Fig.5.** Effect of Grashof number ( $G_r$ ) on temperature profiles.

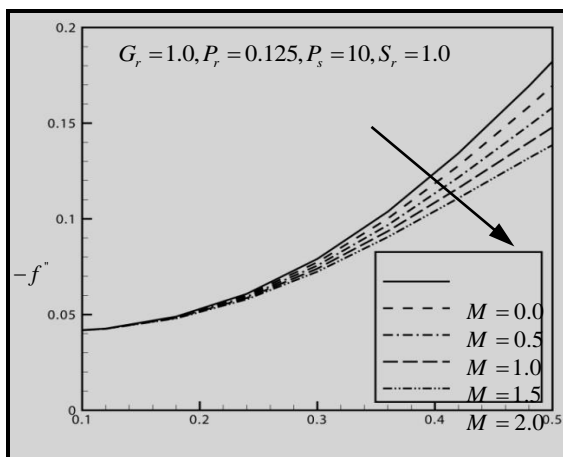


**Fig.6.** Effect of magnetohydrodynamic parameter ( $M$ ) on skin friction coefficient for the vertical plate case ( $\alpha = 90^\circ$ ).

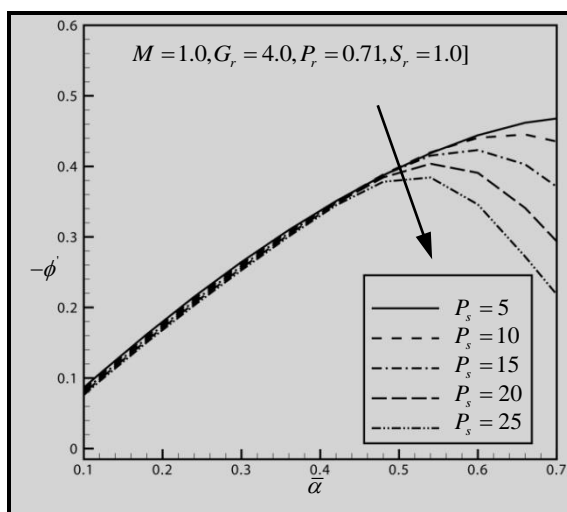


**Fig. 7.** Effect of modified Prandtl number ( $P_s$ ) on salinity transfer rates for the obtuse plate case ( $\alpha = 120^\circ$ ).

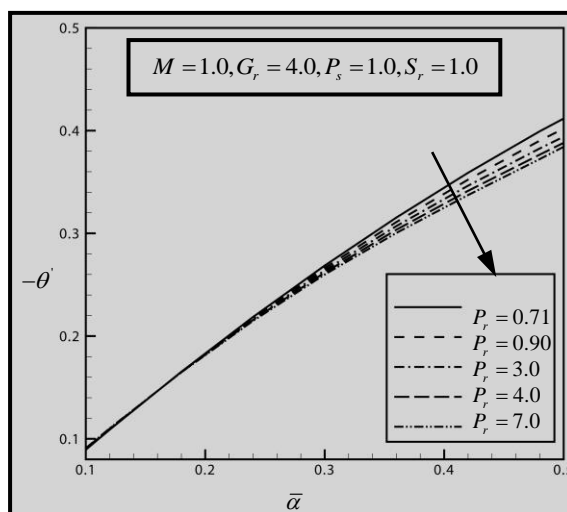


**Fig.8.** Effect of Prandtl number ( $P_r$ ) on heat transfer rates for the obtuse plate case ( $\alpha = 120^\circ$ ).

## 6. CONCLUSIONS

A laminar, steady-state model has been developed for hydromagnetic heat and mass transfer in salt water boundary layer flow from an inclined generator wall (plate) component of an MHD ocean energy generator system. Maple numerical quadrature solutions have been obtained for the normalized two-point boundary value problems. Excellent corroboration of computations has been achieved with the Nakamura implicit finite difference scheme. Further validation has been demonstrated via the Chinese-developed homotopy analysis method (HAM) of Liao. The main findings of the present study may be summarized thus:

- The momentum boundary layer thickness decreases as the Grashof number increase. Also, the skin-friction coefficient decreases as magnetic parameter increases.
- The salinity boundary layer thickness decreases with increasing heat generation parameter increases.
- The thermal boundary layer thickness decreases with increasing Grashof number.
- Salinity transfer rate (Sherwood number function) reduces with increasing modified Prandtl number.
- Surface heat transfer rate (Nusselt number function) decrease as the Prandtl number increases.
- Inclination of the generator wall (plate) exerts a significant effect on all flow characteristics.

The key findings of our study are therefore, that Soret, inclination, mass diffusion (salinity) and heat generation effects *should not be excluded* in MHD ocean generator modelling studies. The computations clearly show that these effects modify the transport phenomena as does inclination of the generator wall (plate). For practical applications, CFD models (e.g. ANSYS FLUENT) while they are geometrically more complex and can simulate 3-dimensional flows, frequently neglect important physical phenomena such as Soret thermo-diffusion and heat generation. MHD simulations we have shown should include both thermal transport and mass (seawater salinity) transport effects. These aspects have been shown to be important and the neglect of mass transfer (salinity), heat generation, thermo-diffusion

would clearly lead to under or over prediction of actual heat and mass transfer characteristics in real MHD ocean generators. Also, the modification in plate orientation which is easily achieved in practical designs (via automatic control) can provide ocean engineers with a useful parameter for modifying the performance of real MHD generators and therefore for controlling the operational efficiency as per the requirements. This may achieve better cost-effectiveness and prove easier in the field relative to other design modifications such as helical MHD generators which are problematic in terms of maintenance and repair. Of course, the analysis has been restricted to two-dimensional flow. Nevertheless, it does provide a good insight into how simpler geometric but more elegant thermophysical formulations can identify important thermofluid characteristics which are neglected in CFD commercial code simulations. The present investigation has however neglected Hall current effects [54-55] and also Joule dissipation effects [56-57]. These are also of relevance in MHD ocean generator systems and are being explored by the authors. Furthermore, the current analysis has been confined to Newtonian flows. The presence of suspensions in seawater may also generate non-Newtonian effects [58-59]. Additionally, nanofluids [60,61] may prove of use in enhancing thermal performance of the working fluids in MHD ocean generator systems. Another possible consideration is the deployment of porous media in the MHD duct [62] and deformable (compliant boundary) duct walls [63]. These aspects are also currently under consideration.

## REFERENCES

- [1] C.N.P. Sze, B.R. Hughes, B.R., O. Anwar Bég, Computational study of improving the efficiency of photovoltaic panels in the UAE. *ICFDT 2011-International Conference on Fluid Dynamics and Thermodynamics, Dubai, United Arab Emirates, January 25-27, 2011.*
- [2] Anwar Bég, O, R.S.R. Gorla, V.R. Prasad, B. Vasu, R.D. Prashad, Computational study of mixed thermal convection nanofluid flow in a geothermal porous medium. *12<sup>th</sup> UK National Heat Transfer Conference, University of Leeds, School of Process Engineering (Energy Institute), 30<sup>th</sup> August - 1<sup>st</sup> September 2011.*
- [3] R.W. Whittlesey, S.C. Liska, J.O. Dabiri, Fish schooling as a basis for vertical-axis wind turbine farm design, *Bioinspiration and Biomimetics*. **5** (2010) 035005.  
[https://doi.org/ 10.1088/1748-3182/5/3/035005](https://doi.org/10.1088/1748-3182/5/3/035005).
- [4] P. McKendry, Energy production from biomass (part 1): overview of biomass. *Bioresource Tech.* 83(1) (2002) 37-46.
- [5] P.K. Takahashi, A. Trenka, *Ocean Thermal Energy Conversion*. UNESCO Energy Engineering Series, John Wiley, USA, 1996.

- [6] M. Grabbe, Marine current energy conversion. *MSc Thesis, Uppsala University, Sweden*, 2008.
- [7] S. Behrens, J. Heyward, M. Hemer, P. Osman, Assessing the wave energy converter potential for Australian coastal regions, *Renewable Energy*. 43 (2011) 210-217.
- [8] S.O. Mathew, O.C. Dike, E.U. Akabuogu, J.N. Ogwo, Magneto-hydrodynamic power generation using salt water, *Asian J. Natural Appl. Sci.* 1(4) (2012) 66-69.
- [9] T.F. Lin, J. B. Gilbert, Studies of helical magnetohydrodynamic seawater flow in fields up to twelve Teslas, *AIAA J. Propulsion and Power*. 11 (1995)1349-1355.
- [10] Y. Peng, Z. Lin, L. Zhao, C. Sha, R. Li, Y. Xu, B. Liu, J. Li, Analysis of Liquid Metal MHD Wave Energy Direct Conversion System. *Proc. 18<sup>th</sup> Int. Offshore and Polar Eng. Conf, Vancouver, BC, Canada, July 6-11, 2008*.
- [11] S.K. Ghosh, O. Anwar Bég, J. Zueco, V.R. Prasad, Transient hydromagnetic flow in a rotating channel permeated by an inclined magnetic field with magnetic induction and Maxwell displacement current effects, *ZAMP: J. Appl. Math. Phys.* 61(2010)147-169.
- [12] E.D. Ross, G.D. Roy, Flow development and analysis of MHD generators and seawater thrusters, *ASME J. Fluids Eng.* 114(1992) 68-72.
- [13] M. Takeda, Y. Okuji, T. Akazawa, X. Liu, T. Kiyoshi, Fundamental studies of helical-type seawater MHD generation system, *IEEE Trans. Appl. Superconductivity*. 15 (2005) 2170-2173.
- [14] M. Takeda, N. Tomomori, T. Akazawa, K. Nishigaki, A. Iwata, Flow control of seawater with a diverging duct by MHD separation method, *IEEE Trans. Appl. Superconductivity*. 14 (2004) 1543-1546.
- [15] G.V.P.N. Srikanth, G. Srinivas, B.R.K. Reddy, MHD convective heat transfer of a nanofluid flow past an inclined permeable plate with heat source and radiation, *Int. J. Phys. Math. Sci.* 3(1) (2013) 89-95.
- [16] G.K. Ramesh, B.J. Gireesha, C.S. Bagewadi, Heat transfer in MHD dusty boundary layer flow over an inclined stretching sheet with non-uniform heat source/sink, *Adv. Math. Phys.* 2012 (2012) 657805-1-657805-13.
- [17] M.A. Kabir, M.A. Al-Mahbub, Effects of thermophoresis on unsteady MHD free convective heat and mass transfer along an inclined porous plate with heat generation in the presence of magnetic field, *Open J. Fluid Dynamics*. 2 (2012) 120-129.
- [18] G. Palani, K.Y. Kim, Joule heating and viscous dissipation effects on MHD flow past a semi-infinite inclined plate with variable surface temperature, *J. Eng. Thermophysics*. 20 (2011) 501-517.
- [19] A.J. Chamkha, C. Issa, K. Khanafer, Natural convection from an inclined plate embedded in a variable porosity porous medium due to solar radiation, *Int. J. Therm. Sci.* 41 (2002) 73-81.
- [20] S. Masthanrao, K.S. Balamurugan, S.V.K. Varma, Chemical reaction effects on MHD free convection flow through a porous medium bounded by an inclined surface, *Int. J. Math. Computer Applic. Research*. 3 (2013) 13-22.
- [21] M.A. Hossain, I. Pop, M. Ahamad, MHD free convection flow from an isothermal plate inclined at a small angle to the horizontal, *J. Theor. Appl. Fluid Mech.* 1 (1996) 194-207.
- [22] H.M. Ramadan, A.J. Chamkha, Hydromagnetic free Convection of a particulate suspension from a permeable inclined plate with heat absorption for non-uniform particle-

- phase density, *Heat and Mass Transfer*. 39 (2003) 367-374.
- [23] C.C. Wang, C.K. Chen, Mixed convection boundary layer flow on inclined wavy plates including the magnetic field effect, *Int. J. Therm. Sci.* 44 (2005) 577-586.
- [24] C.H. Chen, Heat and mass transfer in MHD flow by natural convection from a permeable inclined surface with variable wall temperature and concentration, *Acta Mechanica*. 172 (2004) 219- 235.
- [25] B. Gebhart, *Heat Conduction and Mass Diffusion*, MacGraw-Hill, USA, 1993.
- [26] M. Ferdows, M.J. Uddin, T.S. Khaleque, Double diffusion, slips and variable diffusivity effects on combined heat mass transfer with variable viscosity via a point transformation, *Progress in Computational Fluid Dynamics*. 13(1) (2013) 54-64.
- [27] M.M. Rashidi, N. Rahimzadeh, M. Ferdows, M.J. Uddin, O. Anwar Bég, Group theory and differential transform analysis of mixed convective heat and mass transfer from a horizontal surface with chemical reaction effects, *Chem. Eng. Comm.* 199 (2012)1012-1043.
- [28] J. Zueco, O. Anwar Bég, H.S. Takhar, V.R. Prasad, Thermophoretic hydromagnetic dissipative heat and mass transfer with lateral mass flux, heat source, Ohmic heating and thermal conductivity effects: network simulation numerical study, *Appl. Therm. Eng.* 29 (2009) 2808-2815.
- [29] O.D. Makinde, K. Zimba, O. Anwar Bég, Numerical study of chemically-reacting hydromagnetic boundary layer flow with Soret/Dufour effects and a convective surface boundary condition, *Int. J. Therm. Env. Eng.* 4 (2012) 89-98.
- [30] C.R.A. Abreu, M.F. Alfradique, A.S. Telles, Boundary layer flows with Dufour and Soret effects: I- Forced and natural convection, *Chem. Eng. Sci.* 61 (2006) 4282-4289.
- [31] O. Anwar Bég, A.Y. Bakier, V.R. Prasad, S.K. Ghosh, Numerical modelling of non-similar mixed convection heat and species transfer along an inclined solar energy collector surface with cross diffusion effects, *World J. Mech.* 1 (2011) 185-196.
- [32] O. Anwar Bég, D. Tripathi, Mathematica simulation of peristaltic pumping with double-diffusive convection in nanofluids: a bio-nano-engineering model, *Proc. IMechE. Part N: J. Nanoengineering Nanosystems*. 225 (2012) 99–114.
- [33] R.M.L. Coelho, A.S. Telles, Extended Graetz problem accompanied by Dufour and Soret effects, *Int. J. Heat Mass Transfer*. 45 (2002) 3101-3110.
- [34] O. Anwar Bég, A.Y. Bakier, V.R. Prasad, Numerical study of free convection magnetohydrodynamic heat and mass transfer from a stretching surface to a saturated porous medium with Soret and Dufour effects, *Comput. Mat. Sci.* 46 (2009a) 57-65.
- [35] O. Anwar Bég, R. Bhargava, S. Rawat, E. Kahya, Numerical study of micropolar convective heat and mass transfer in a non-Darcian porous regime with Soret/Dufour diffusion effects, *Emir. J. Eng. Research*. 13 (2008) 51-66.
- [36] B. Vasu, V.R. Prasad, O. Anwar Bég, Thermo-diffusion and diffusion-thermo effects on MHD free convective heat and mass transfer from a sphere embedded in a non-Darcian porous medium, *J. Thermodynamics*. 2012 (2012) 725142-1-725142-17.
- [37] B. Vasu, O. Anwar Bég, N.B. Reddy, V.R. Prasad, Thermo-diffusion and diffusion-thermo effects on free convection flow past a semi-infinite vertical plate in the presence of suction and injection, *Int. J. Energy and Tech.* 14(5) (2013) 1-11.
- [38] O. Anwar Bég, J. Zueco, R. Bhargava, H.S. Takhar, Magnetohydrodynamic convection

flow from a sphere to a non-Darcian porous medium with heat generation or absorption effects: network simulation, *Int. J. Therm. Sci.* 48 (2009b) 913-921.

- [39] M.J. Uddin, N.H.M. Yusoff, O. Anwar Bég, A.I.M. Ismail, Lie group analysis and numerical solutions for non-Newtonian nanofluid flow in a porous medium with internal heat generation, *Phys. Scr.* 87 (2013)1-14.
- [40] S. Nakamura, Iterative finite difference schemes for similar and non-similar boundary layer equations, *Adv. Eng. Software.* 21 (1994) 123-130.
- [41] B. Gebhart *et al.*, *Buoyancy-Induced Flows and Transport*, Hemisphere Pub. Corp., Washington, USA (1988).
- [42] P.R. Nachtsheim, P. Swigert, Satisfaction of the asymptotic boundary conditions in numerical solution of the system of non-linear equations of boundary layer type. NASA TND-3004, USA, 1965.
- [43] R. J. Rosa. *Magnetohydrodynamic Energy Conversion*, Hemisphere Pub. Corp, rev. print edition, Washington, USA (1987).
- [44] X. Li *et al.*, Simulation of a seawater MHD power generation system, *Cryogenics*, 46, 362-366 (2006).
- [45] O. Anwar Bég, Numerical methods for multi-physical magnetohydrodynamics, Ch.1, pp. 1-110, *New Developments in Hydrodynamics Research*, (Eds: Maximiano J. Ibragimov and Miroslava A. Anisimov), Nova Science, New York, USA, 2012.
- [46] R.S.R. Gorla, A. Slaouti, H.S. Takhar, Free convection in micropolar fluids over a uniformly heated vertical plate, *Int. J. Num. Meth. Heat Fluid Flow.* 8 (1998a) 504- 518.
- [47] R.S.R. Gorla, H.S. Takhar, A. Slaouti, Magnetohydrodynamic free convection boundary layer flow of a thermo-micropolar fluid over a vertical plate, *Int. J. Eng. Sci.* 36 (1998b), 315-327.
- [48] O. Anwar Bég, T.A. Bég, Nakamura tridiagonal difference scheme for electromagnetic control of ionized diffusion flames. *Technical Report-FireMod-4-3-06*, 87 pages, *Leeds Metropolitan University, Leeds*, 2006.
- [49] O. Anwar Bég, V.R. Prasad, B. Vasu, Numerical study of mixed bioconvection in porous media saturated with nanofluid containing oxytactic micro-organisms, *J. Mech. Med. Biol.* 13(4) (2013) 1350067.1-1350067.25.
- [50] S.J. Liao, *Beyond Perturbation: Introduction to the Homotopy Analysis Method*, CRC Press, Boca Raton, Florida, USA, 2003.
- [51] O. Anwar Bég, M.M. Rashidi, T.A. Bég, M. Asadi, Homotopy analysis of transient magneto-bio-fluid dynamics of micropolar squeeze film: a model for magneto-bio-rheological lubrication, *J. Mech. Med. Biol.* 12(3) (2012) 1250051-1 to 1250051-21.
- [52] T.A. Bég, O. Anwar Bég, M.M. Rashidi, M. Asadi, Homotopy semi-numerical modelling of nanofluid convection flow from an isothermal spherical body in a permeable regime, *Int. J. Microscale Nanoscale Thermal and Fluid Transport Phenomena.* 3(4) (2012c) 67-96.
- [53] M. Haajizadeh, A.F. Ozguc, C.L. Tien, Natural convection in vertical porous enclosure with internal heat generation, *Int. J. Heat Mass Transfer.* 27 (1984) 1893-1902.
- [54] O. Anwar Bég, L. Sim, J. Zuco, R. Bhargava, Numerical study of magnetohydrodynamic viscous plasma flow in rotating porous media with Hall currents and inclined magnetic field influence, *Commun. Nonlinear Sci. Numer. Sim.* 15 (2010) 345–359.
- [55] L.P. Harris, J.D. Cobine, The significance of the Hall effect for three MHD generator configurations, *ASME J. Energy for Power (A).* 83(4) (1961) 392-396.
- [56] MD. Shamshuddin, S.R. Mishra, O. Anwar Bég, A. Kadir, Unsteady reactive magnetic radiative micropolar flow, heat and mass transfer from an inclined plate with Joule heating: a model for magnetic polymer processing. *Proc. IMechE- Part C: Mech. Eng. Sci.* (2018).

<https://doi.org/10.1177/0954406218768837>.

[57] R.K. James, C.H. Kruger, Joule heating effects in MHD generators boundary layers, *AIAA J.* 21(1983) 679-686.

[58] Kai-Long Hsiao, To promote radiation electrical MHD activation energy thermal extrusion manufacturing system efficiency by using Carreau-nanofluid with parameters control method, *Energy*, 130 (2017) 486-499.

[59] Kai-Long Hsiao, Combined electrical MHD heat transfer thermal extrusion system using Maxwell fluid with radiative and viscous dissipation effects, *Applied Thermal Engineering*, 112, 1281-1288 (2017).

[60] Kai-Long Hsiao, Micropolar nanofluid flow with MHD and viscous dissipation effects towards a stretching sheet with multimedia feature, *International Journal of Heat and Mass Transfer*, 112 (2017) 983–990.

[61] Kai-Long Hsiao, Stagnation electrical MHD Nanofluid mixed convection with slip boundary on a stretching sheet, *Applied Thermal Engineering*, 98, 850-861 (2016).

[62] M. Turkyilmazoglu, MHD natural convection in saturated porous media with heat generation/absorption and thermal radiation. *Achieves of Mechanics*, 71: 49-64 (2019).

[63] M. Turkyilmazoglu, Analytical solutions to mixed convection MHD fluid flow induced by a nonlinearly deforming permeable surface. *Communications in Nonlinear Science and Numerical Simulation*, 63: 373-379 (2018).